Large Eddy Simulation with Unstructured High-Order Numerical Methods for Real-World Turbulent Flows

Jonathan R. Bull

Postdoctoral Research Scholar
Aerospace Computing Laboratory (ACL)
Department of Aeronautics and Astronautics
Stanford University
Advisor: Professor Antony Jameson

NASA AMS Seminar
November 7th 2013

The Aerospace Computing Lab

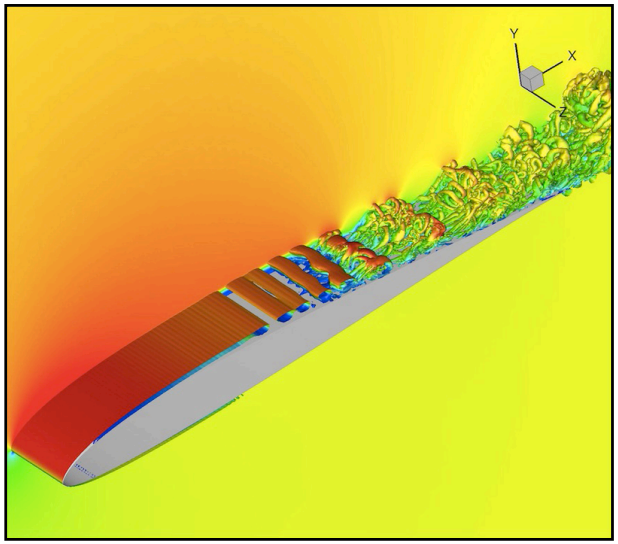

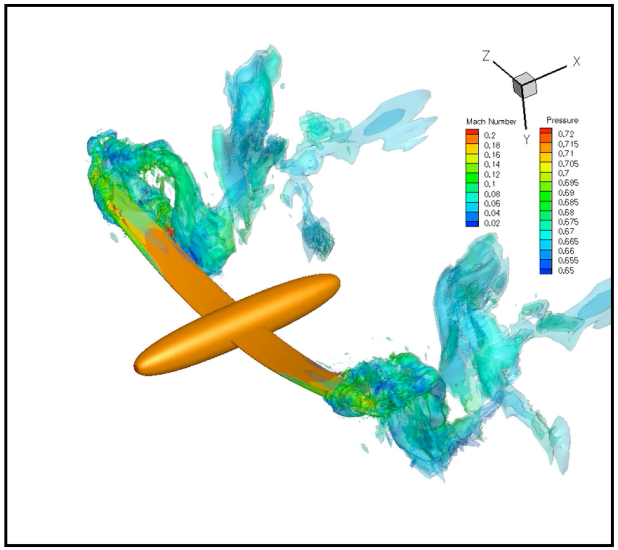

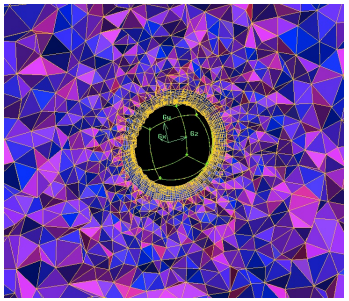

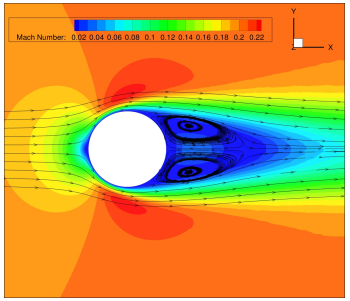

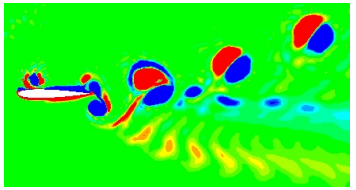

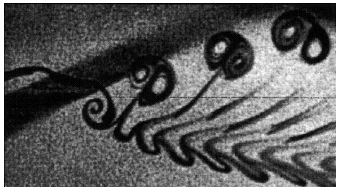

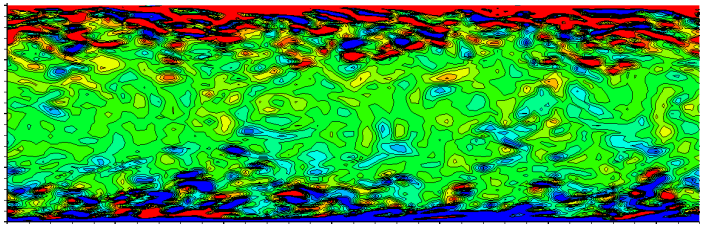

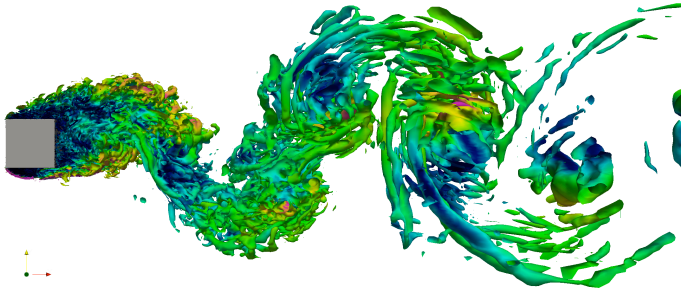

Speaker Profile

- May 2013: Joined Prof. Antony Jameson's Aerospace Computing Laboratory (ACL)
  - Combining large-eddy simulation (LES) with high-order discontinuous numerical methods
- March 2013: Completed PhD at Imperial College London, UK
  - Joint project with Applied Modelling and Computation Group (AMCG) and Rolls-Royce Submarines
  - Developed RANS & LES turbulence modelling in finite element code 'Fluidity' featuring unstructured adaptive meshing
- 2007: Masters in Mechanical Engineering from University of Manchester, UK

Motivation

- Features of real-world turbulent flows:
  - Complex geometry
  - Very high Reynolds numbers ($Re > 10^7$)
  - Separation, reattachment, vortex interactions
  - Importance of small scales e.g. aeroacoustics
- Need unstructured meshes to fit geometry
- Need LES to make accurate predictions of complex phenomena at high Re
- Need high-order methods to reduce numerical error at small scales

- L: rotor-vortex interaction, M: high-lift wing, R: jet stalling

Outline

Introduction

High-Order Discontinuous Numerical Schemes

High-Order LES
- Advanced SGS Models
- Discrete Filters
- Current Work

Summary and Future Directions

LES On Unstructured Meshes

- Easier to fit to complex geometry
- Easier to vary resolution
- Fewer degrees of freedom

LES On Unstructured Meshes

- Easier to fit to complex geometry
- Easier to vary resolution
- Fewer degrees of freedom

- $Re = 5100$
- 2nd order finite element code Fluidity
- Tetrahedral mesh, 250k elements
- Adaptive meshing
- Dynamic LES
- Reattachment length within 4% of DNS
- Greater accuracy with 60% fewer elements vs. structured mesh

Bull et al (2012), Turbulent Heat and Mass Transfer 7.

Backward-Facing Step

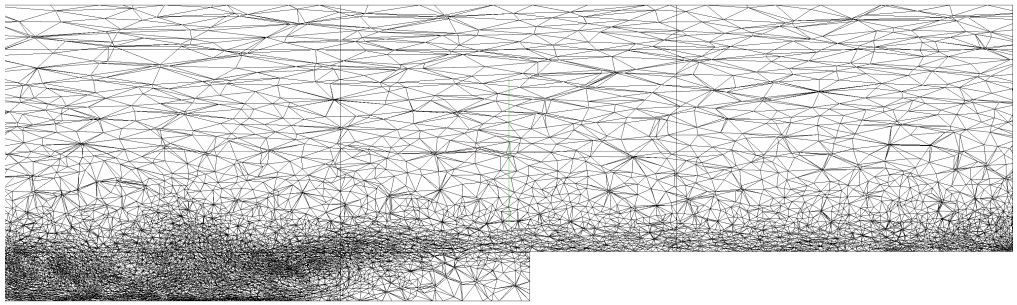

slice through mesh on midplane

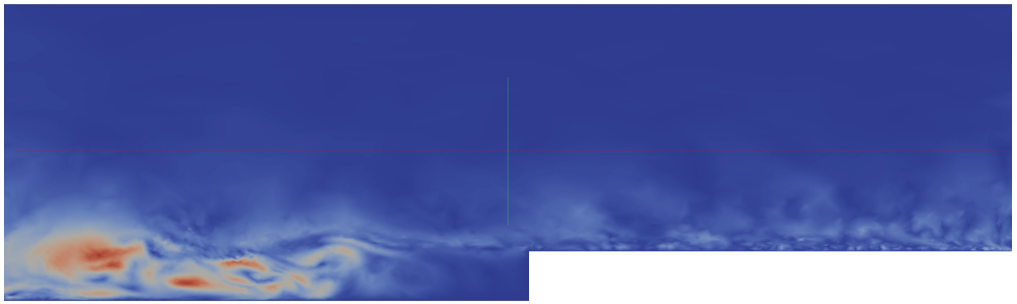

Reynolds stress magnitude on midplane

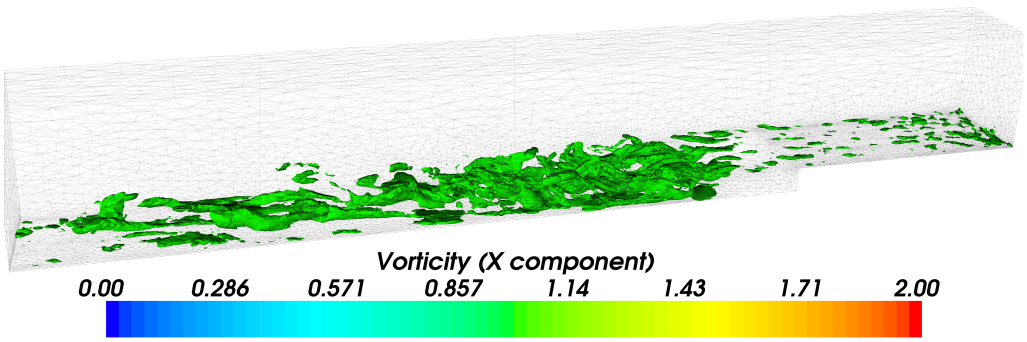

vorticity isosurface

High-Order Discontinuous Numerical Methods

- Many applications where resolution of small scales is important
- 2nd-order schemes: highly dissipative, errors in small scales
- High order (> 2): lower dissipation, improved small-scale resolution
- Discontinuous high-order schemes have local stencil: efficient parallelisation
- Greater accuracy per degree of freedom (DoF)

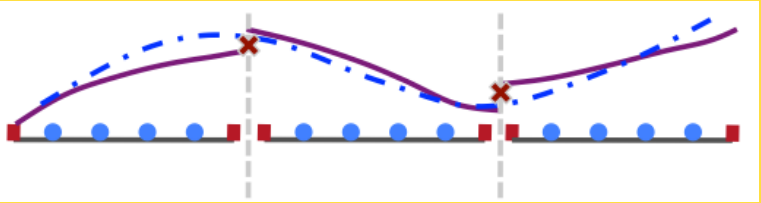

- Blue dash-dot: exact solution; purple: discrete representation by second-order finite volume (L) and high-order discontinuous Galerkin (R) schemes. Dots are solution points (DoF).

High-Order Flux Reconstruction (FR) Schemes

- Discretise u, f using degree $N-1$ Lagrange polynomials at N solution points:

$$u_h^D = \sum_{j=1}^{N} u_j l_j(\xi), \quad f_h^D = \sum_{j=1}^{N} f_j^D l_j(\xi), \quad \xi \in [-1:1]$$

- u_h^D, f_h^D discontinuous across element interfaces

1. Represent u, f by Lagrange polynomial of degree $N-1$ in element

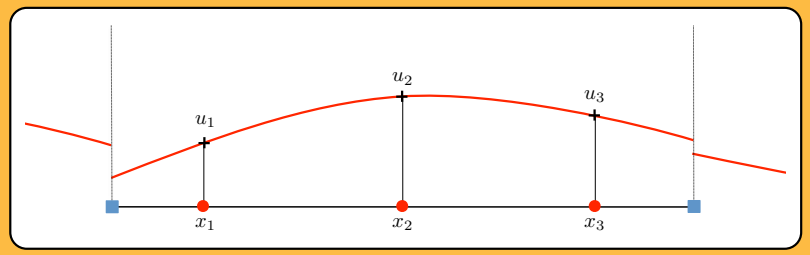

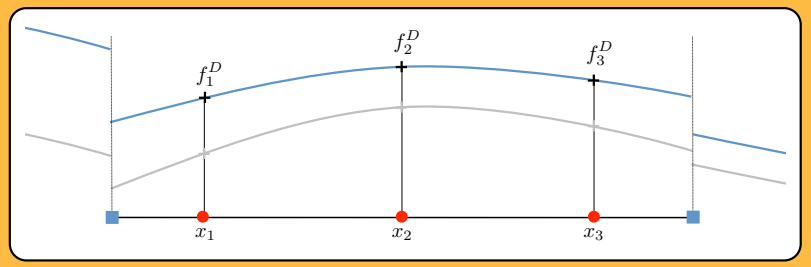

Huynh (2007) AIAA P., 2007-4079

High-Order Flux Reconstruction (FR) Schemes

- Compute common interface fluxes $\tilde{f}_L, \tilde{f}_R$, e.g. Roe flux method

Huynh (2007) AIAA P., 2007-4079

High-Order Flux Reconstruction (FR) Schemes

- Compute common interface fluxes $\tilde{f}_L, \tilde{f}_R$, e.g. Roe flux method

2. Get common interface fluxes $\tilde{f}_L, \tilde{f}_R$

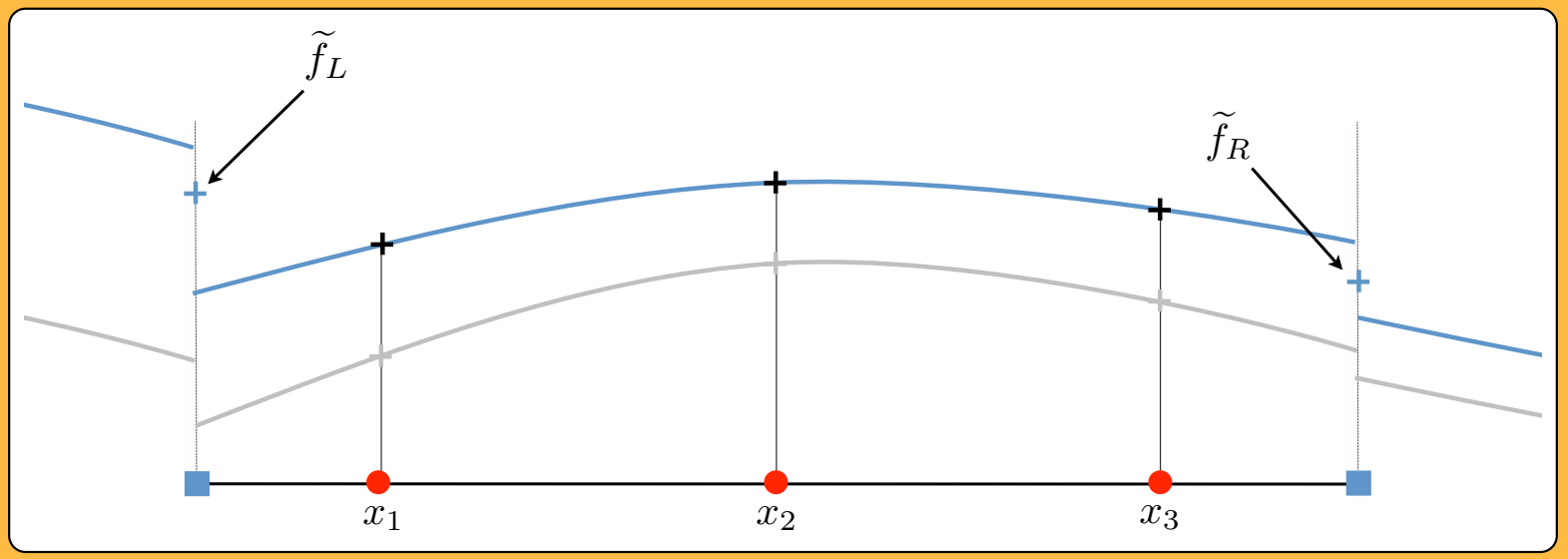

Huynh (2007) AIAA P., 2007-4079

High-Order Flux Reconstruction (FR) Schemes

- correction functions g_L, g_R satisfying:

$$g_L(-1) = g_R(1) = 1, \quad g_L(1) = g_R(-1) = 0, \quad g_L(\xi) = g_R(-\xi),$$

3. Correction function g_L

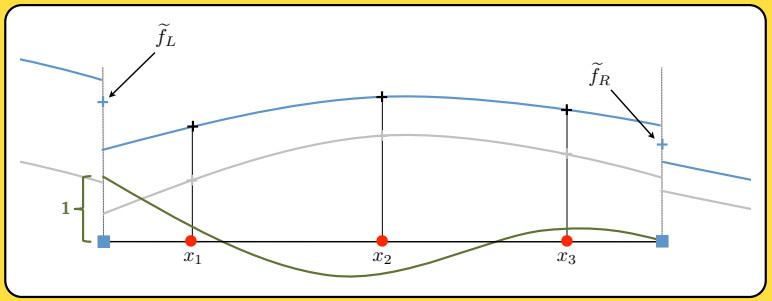

Huynh (2007) AIAA P., 2007-4079

High-Order Flux Reconstruction (FR) Schemes

- correction functions g_L, g_R satisfying:

$$g_L(-1) = g_R(1) = 1, \quad g_L(1) = g_R(-1) = 0, \quad g_L(\xi) = g_R(-\xi),$$

- Weight by flux corrections Δ_L, Δ_R:

$$\Delta_L = \tilde{f}_L - f_h^D(-1), \quad \Delta_R = \tilde{f}_R - f_h^D(1)$$

3. Correction function g_L

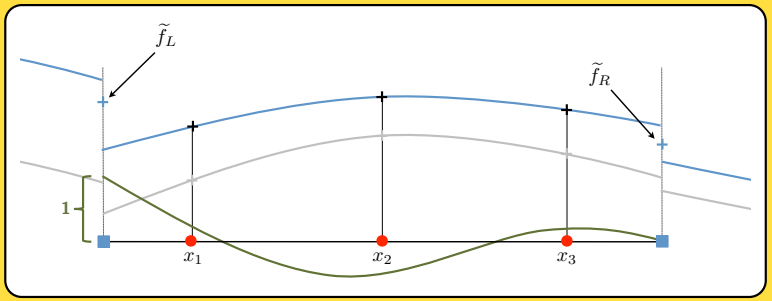

4. Scale correction function g_L by $\triangle_L$

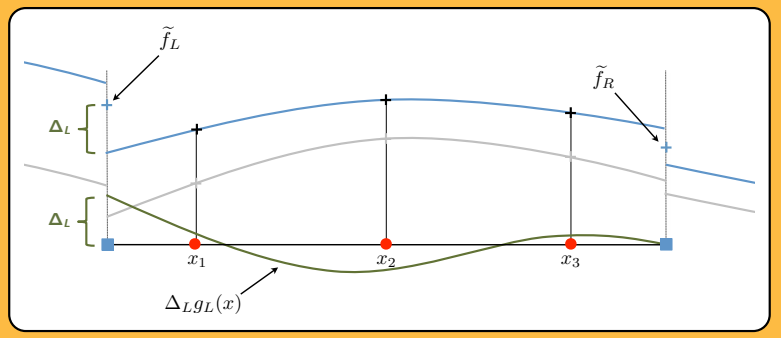

Huynh (2007) AIAA P., 2007-4079

High-Order Flux Reconstruction (FR) Schemes

5. Add scaled correction to f_D

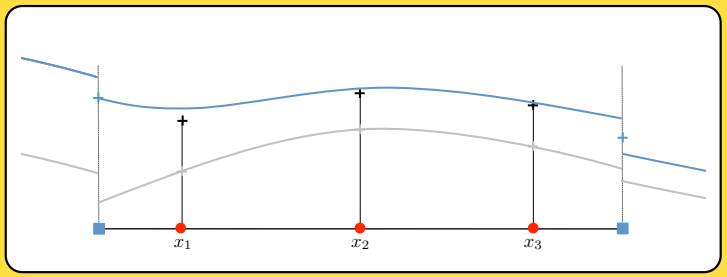

Huynh (2007) AIAA P., 2007-4079

High-Order Flux Reconstruction (FR) Schemes

5. Add scaled correction to f_D

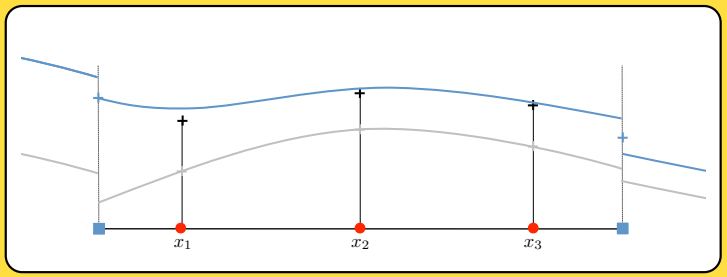

6. Do steps 3-5 on right interface

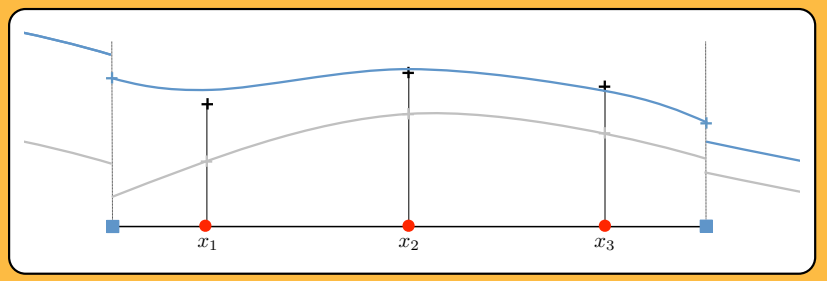

Huynh (2007) AIAA P., 2007-4079

High-Order Flux Reconstruction (FR) Schemes

5. Add scaled correction to f_D

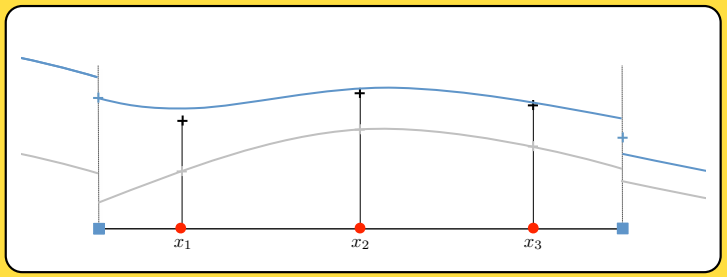

6. Do steps 3-5 on right interface

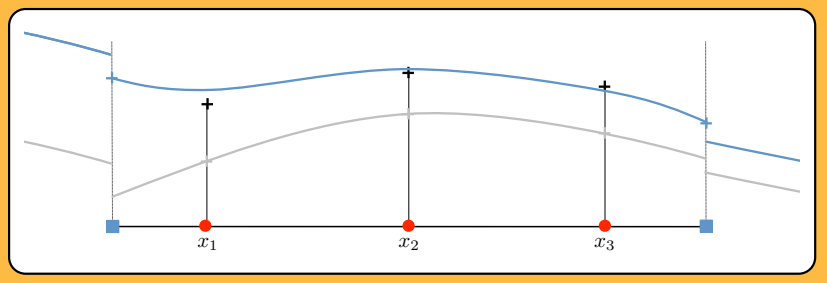

7. Globally C_0-continuous flux f_C

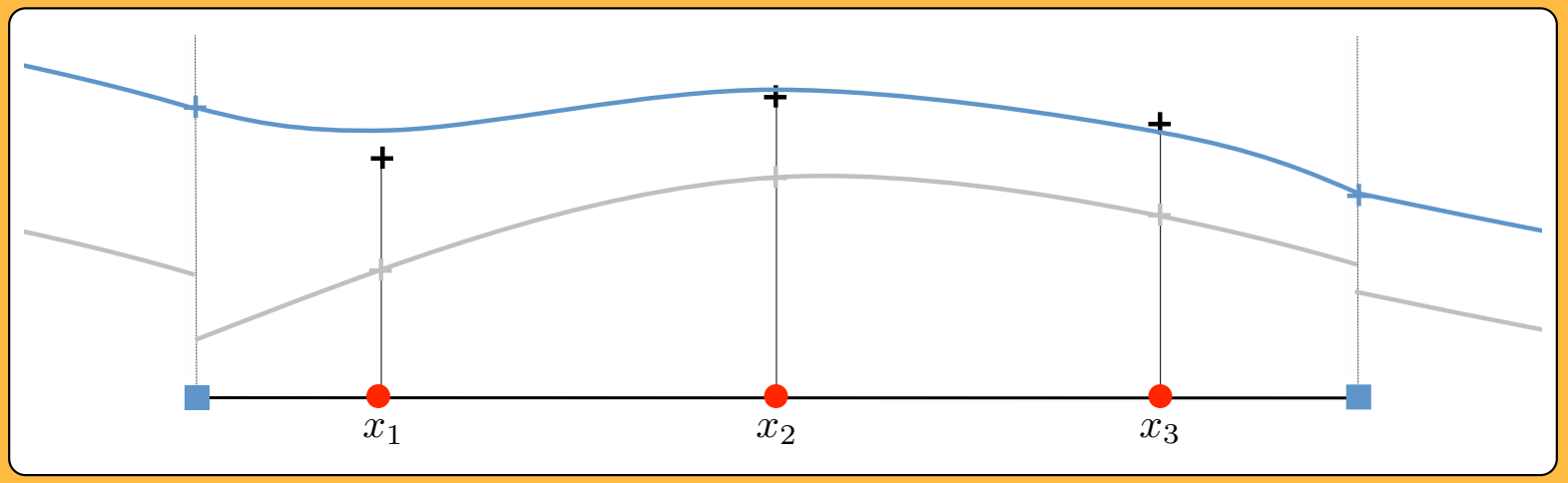

Huynh (2007) AIAA P., 2007-4079

High-Order Flux Reconstruction (FR) Schemes

8. Differentiate continuous flux at solution points and advance solution in time:

$$\frac{\partial f^C}{\partial x}(x_i) = \sum_{j=1}^{n} f_j^D \frac{\mathrm{d}l_j}{\mathrm{d}x}(x_i) + \Delta_L \frac{\mathrm{d}g_L}{\mathrm{d}x}(x_i) + \Delta_R \frac{\mathrm{d}g_R}{\mathrm{d}x}(x_i)$$

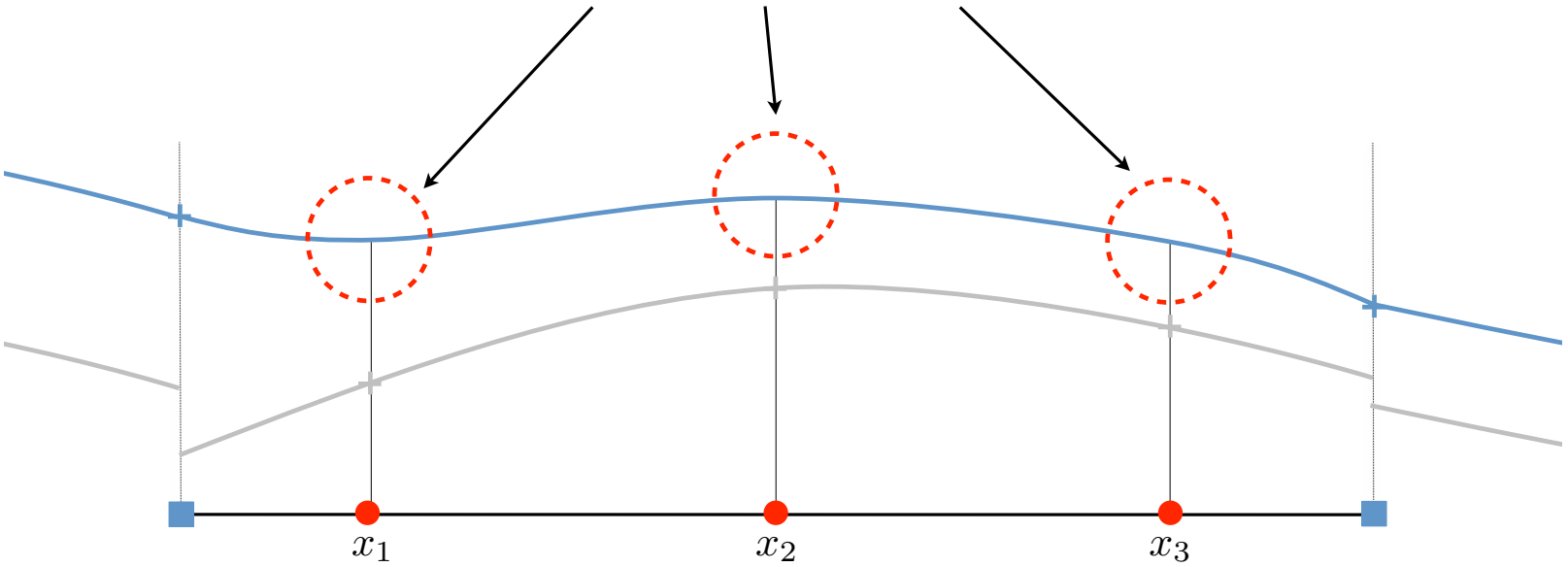

Huynh (2007) AIAA P., 2007-4079

Energy-Stable FR Schemes

- Scheme is energy-stable (for linear f) if energy norm does not increase in time:

$$\frac{d}{dt}\|u_h\|_{p,2}^2 = \frac{d}{dt}\left[\sum_{n=0}^{N-1}\int_{x_n}^{x_{n+1}} u_{h,n}^2 + \frac{c}{2}(J_n)^{2p}\left(\frac{\partial^p u_{h,n}}{\partial x^p}\right)^2 dx\right]^{1/2} \leq 0, \quad (1)$$

Vincent, et al. (2010). J. Sci. Comput., 47(1)

Energy-Stable FR Schemes

- Scheme is energy-stable (for linear f) if energy norm does not increase in time:

$$\frac{d}{dt}\|u_h\|_{p,2}^2 = \frac{d}{dt}\left[\sum_{n=0}^{N-1}\int_{x_n}^{x_{n+1}} u_{h,n}^2 + \frac{c}{2}(J_n)^{2p}\left(\frac{\partial^p u_{h,n}}{\partial x^p}\right)^2 dx\right]^{1/2} \leq 0, \quad (1)$$

- Choose correction functions g_L, g_R to satisfy (1):

$$g_L = \frac{(-1)^p}{2}\left[L_p - \left(\frac{\eta_p(c)L_{p-1} + L_{p+1}}{1+\eta_p(c)}\right)\right],$$

$$g_R = \frac{(-1)^p}{2}\left[L_p - \left(\frac{\eta_p(c)L_{p-1} + L_{p+1}}{1+\eta_p(c)}\right)\right],$$

- L_p = Legendre polynomial, $\eta_p(c) = (c(2p+1)(a_p p!))^2)/2$

Vincent, et al. (2010). J. Sci. Comput., 47(1)

Energy-Stable FR Schemes

- Scheme is energy-stable (for linear f) if energy norm does not increase in time:

$$\frac{d}{dt}\|u_h\|_{p,2}^2 = \frac{d}{dt}\left[\sum_{n=0}^{N-1}\int_{x_n}^{x_{n+1}} u_{h,n}^2 + \frac{c}{2}(J_n)^{2p}\left(\frac{\partial^p u_{h,n}}{\partial x^p}\right)^2 dx\right]^{1/2} \leq 0, \quad (1)$$

- Choose correction functions g_L, g_R to satisfy (1):

$$g_L = \frac{(-1)^p}{2}\left[L_p - \left(\frac{\eta_p(c)L_{p-1} + L_{p+1}}{1+\eta_p(c)}\right)\right],$$

$$g_R = \frac{(-1)^p}{2}\left[L_p - \left(\frac{\eta_p(c)L_{p-1} + L_{p+1}}{1+\eta_p(c)}\right)\right],$$

- L_p = Legendre polynomial, $\eta_p(c) = (c(2p+1)(a_p p!))^2)/2$

- Family of energy-stable schemes known as VCJH Schemes

Vincent, et al. (2010). J. Sci. Comput., 47(1)

A Family of Energy-Stable Schemes

- Nonlinear flux: aliasing instability
- Set $c > 0$ to damp instability (similar to filtered Discontinuous Galerkin (DG))
- Choose c to compromise between (1) accuracy, (2) damping, (3) CFL limit
- Choose Gauss-Legendre points as solution points to minimise aliasing error

Effect of c on damping of aliasing instability

c	Scheme	Damping
0	nodal DG	no damping
$\frac{2p}{(2p+1)(p+1)(p!a_p)^2}$	Spectral Difference	damped
$\frac{2(p+1)}{(2p+1)p(p!a_p)^2}$	g_2 (Huynh 2007)	damped
tabulated[1]	$c+$	damped
$\rightarrow \infty$	–	totally damped

[1] Determined experimentally for each order p and RK timestepping scheme

Vincent, et al. (2011). J. Comput. Phys., 230(22)

Taylor-Green Vortex at Re $= 1600$

- Analytical solution develops into turbulent spectrum in prescribed manner
- Allows quantification of numerical dissipation

Isosurfaces of z-component of vorticity at $t = 0$ *(L) and* $t = 20$ *(R)*

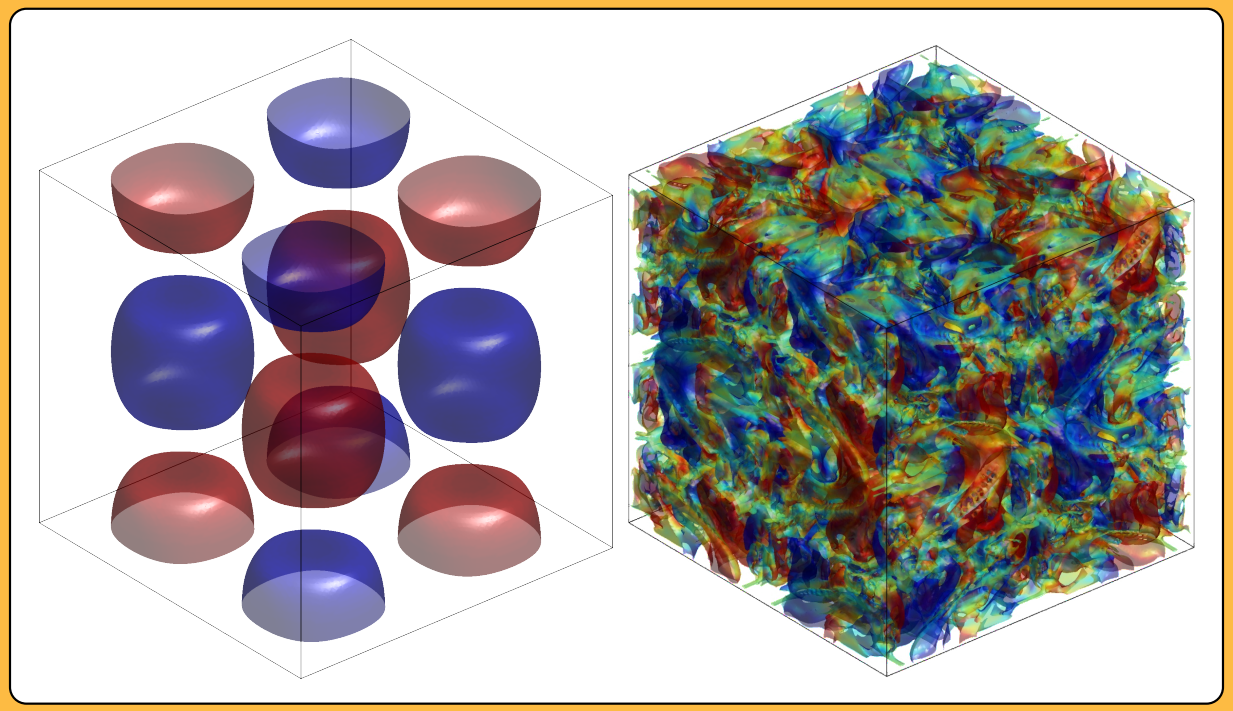

ONERA benchmark solution (2012)

Taylor-Green Vortex at Re = 1600

- 4th order accurate SD on hex meshes: 16^3, 32^3, 64^3 elements
- Comparing to 4th order filtered DG (Beck and Gassner (2013)), DNS (Debonis (2012))

Average kinetic energy $\langle k \rangle = \frac{1}{V}\int k dV$

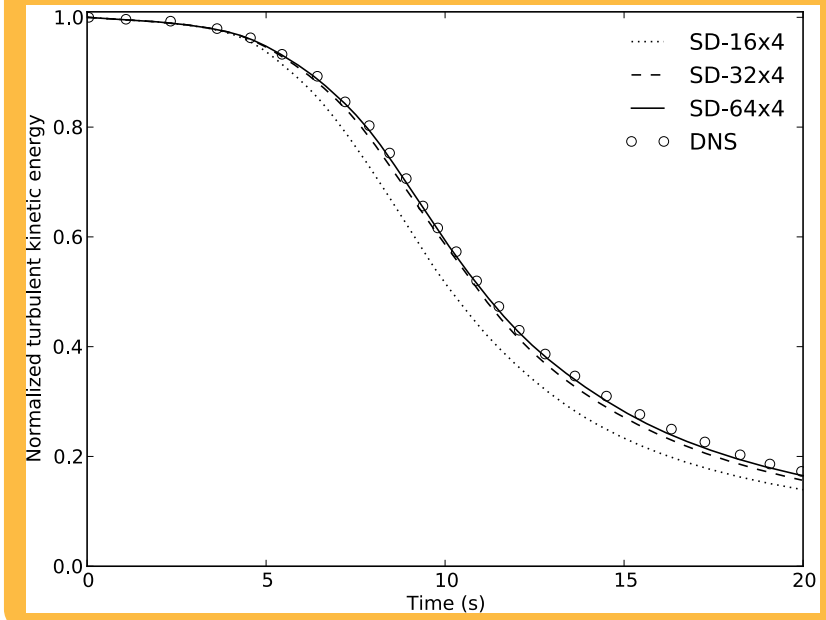

Dissipation rate $-d/dt(\langle k \rangle)$

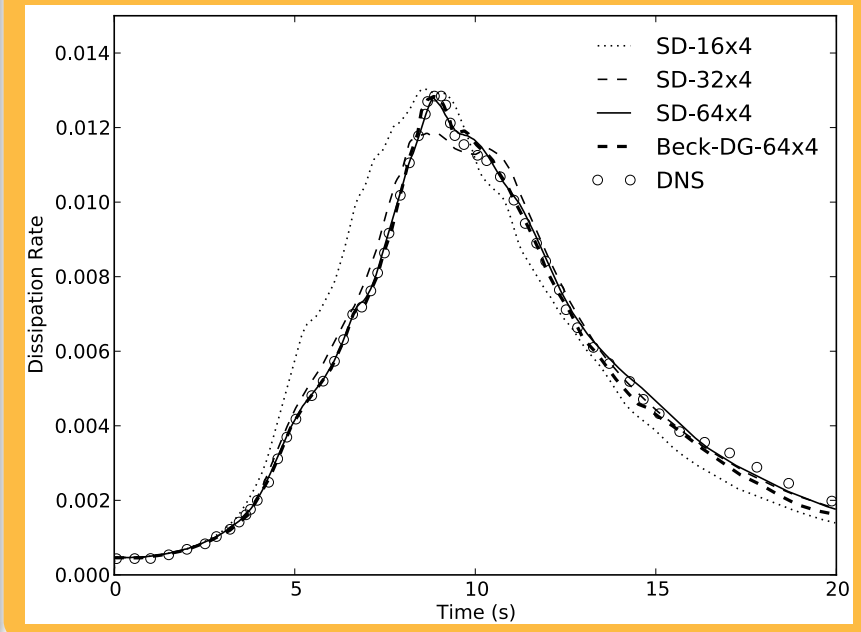

Taylor-Green Vortex - Tetrahedral Meshes

- Tetrahedral meshes formed by splitting hex elements
- Identical results to hex meshes

Average kinetic energy $\langle k \rangle = \frac{1}{V} \int k dV$

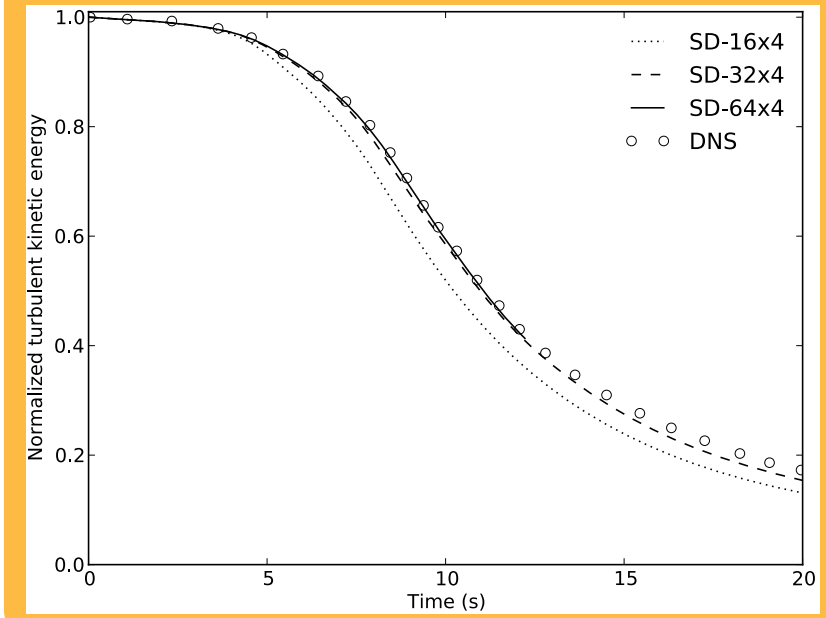

Dissipation rate $-d/dt(\langle k \rangle)$

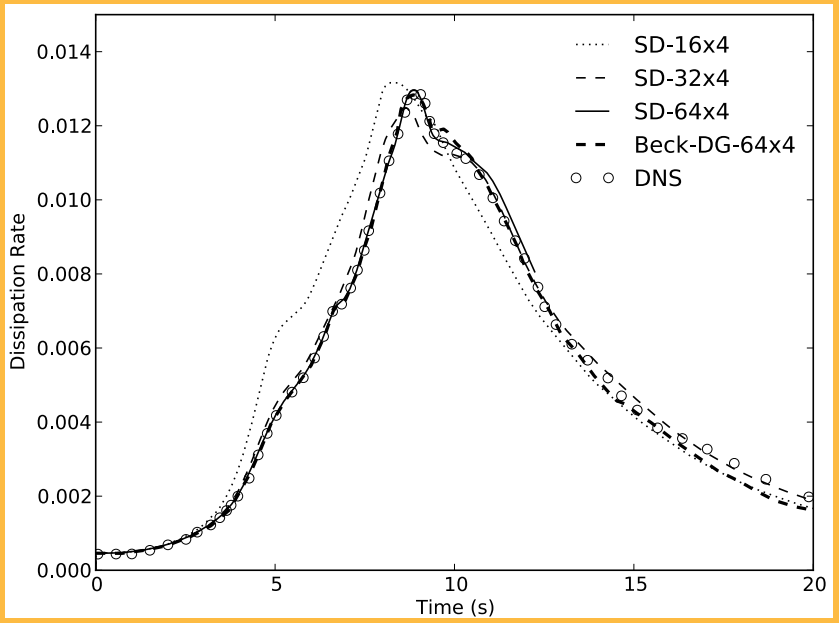

Taylor-Green Vortex - Effect of Scheme Order

- 3rd - 7th/6th order accurate SD on 16^3 hex/tet meshes
- Same results with g_2 scheme (Huynh 2007)
- Aliasing instability appears for > 5 order on hexes
- Odd/even disparity, predicted by Jameson and Lodato (2013)

Dissipation rate - hex mesh

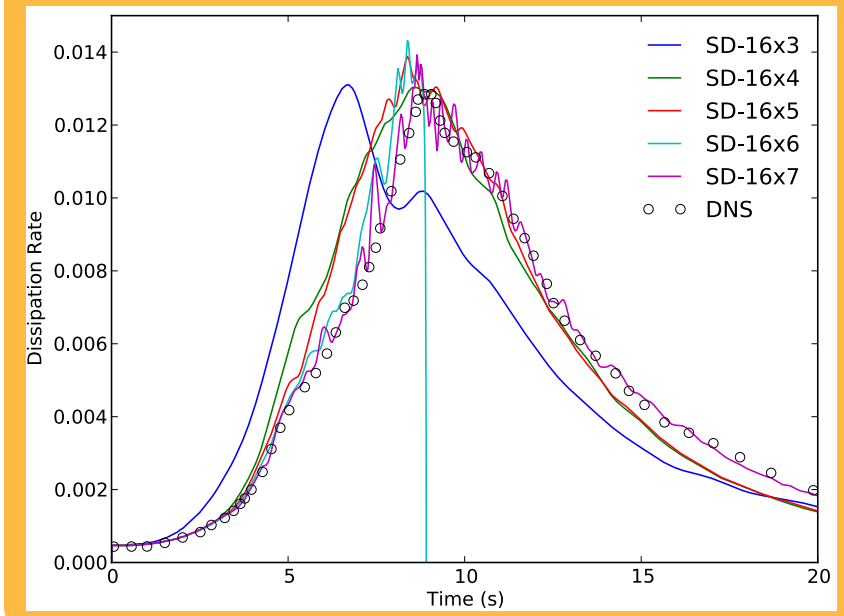

Dissipation rate - tet mesh

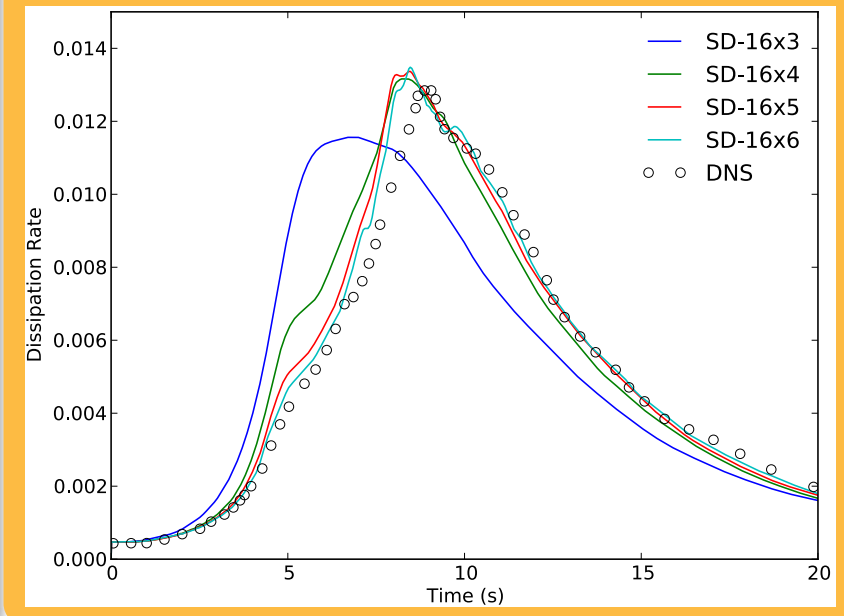

Spectral Difference Applied to Separated Turbulent Flows

- *L to R:* SD7003 airfoil (Q-criterion isosurfaces, $Re = 6 \times 10^4$); sphere (vorticity isosurfaces, $Re = 1 \times 10^4$); flapping wing-body (entropy isosurfaces, $Re = 5000$)

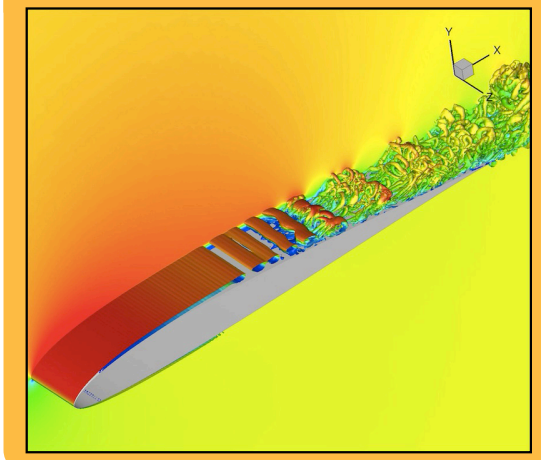

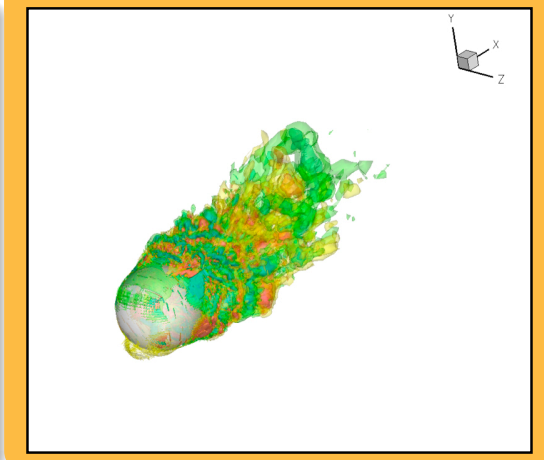

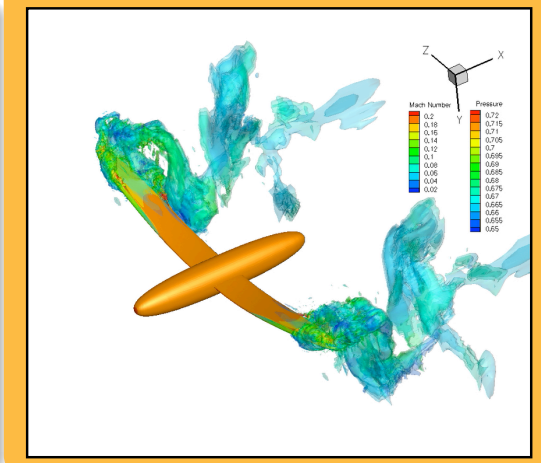

Castonguay, et al. (2010), AIAA P., 2010-4626. Ou, et al. (2011), AIAA P., 2011-3668. Ou, Jameson (2011), AIAA P., 2011-3068.

Spectral Difference Applied to Separated Turbulent Flows

- *L to R:* SD7003 airfoil (Q-criterion isosurfaces, $Re = 6 \times 10^4$); sphere (vorticity isosurfaces, $Re = 1 \times 10^4$); flapping wing-body (entropy isosurfaces, $Re = 5000$)

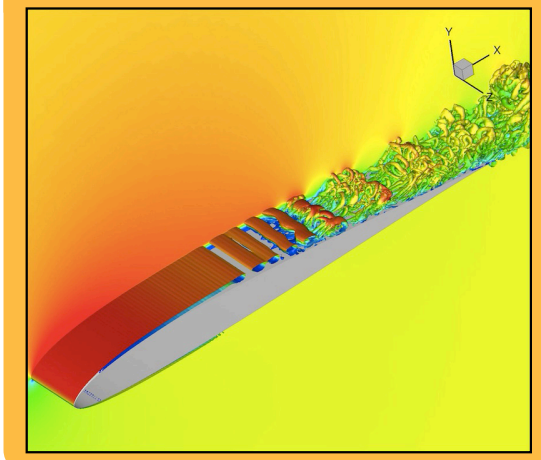

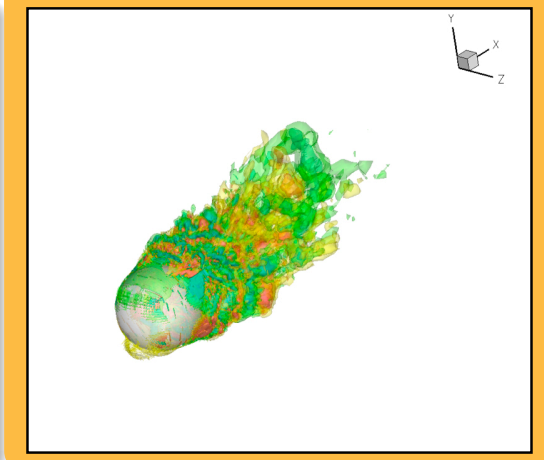

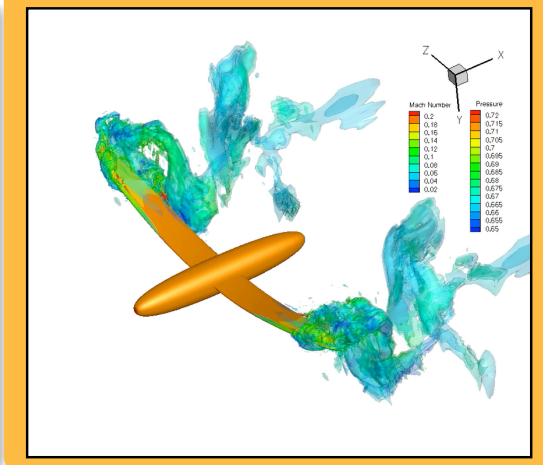

- Numerical dissipation sufficient to stabilise separated flows at moderate Re
- Wider range of scales at real-world conditions ($Re > 10^7$)
- Under-resolution is inevitable - numerical dissipation insufficient
- Need SGS model to increase accuracy and stability

Castonguay, et al. (2010), AIAA P., 2010-4626. Ou, et al. (2011), AIAA P., 2011-3668. Ou, Jameson (2011), AIAA P., 2011-3068.

Advanced Subgrid-Scale (SGS) Models

(a) Functional SGS models: pure dissipation, e.g. eddy-viscosity
(b) Structural SGS models: recreation of SGS stress tensor, e.g. Similarity

- Mixed models combine advantages of functional and structural models
- Dynamic models scale functional model to suit local flow conditions

[1] Lodato et al. (2009), Phys. Fl, 21(3). [2] Moin et al. (1991), Phys. Fl. A. (3).

Advanced Subgrid-Scale (SGS) Models

(a) Functional SGS models: pure dissipation, e.g. eddy-viscosity
(b) Structural SGS models: recreation of SGS stress tensor, e.g. Similarity

- Mixed models combine advantages of functional and structural models
- Dynamic models scale functional model to suit local flow conditions

- WALE-Similarity Mixed Model (WSM)[1]:

$$\tau_{ij} = 2\overline{\rho}[\underbrace{\nu_t \tilde{S}_{ij}}_{\text{(a) WALE Eddy Viscosity}} - \underbrace{(\widehat{\tilde{u}_i\tilde{u}_j} - \widehat{\tilde{u}}_i\widehat{\tilde{u}}_j)}_{\text{(b) Similarity}}]$$

- Compressible dynamic eddy-viscosity model[2]:

$$\nu_t = C_S^2(\mathbf{x},t)\overline{\triangle}^2|\tilde{S}|, \quad C_s(\mathbf{x},t) = f\left(\widehat{\tilde{u}_i\tilde{u}_j}, \widehat{\tilde{u}}_i\widehat{\tilde{u}}_j, |\widehat{\tilde{S}}|\widehat{\tilde{S}}_{ij}\right)$$

- $\tilde{g} = \overline{\rho g}/\overline{\rho}$ = Favre-filtered quantity, $\widehat{\tilde{g}} = F(\tilde{g})$ = explicitly filtered quantity
- Explicit filter F filters out resolved scales $L \leq \widehat{\triangle}$
- Nature of F is critical to model behaviour and accuracy

[1] Lodato et al. (2009), Phys. Fl, 21(3). [2] Moin et al. (1991), Phys. Fl. A. (3).

Types of Filter

2D Filter kernels

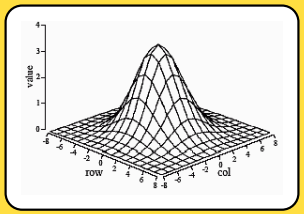

Gaussian

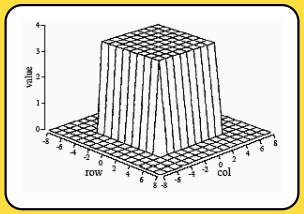

Box

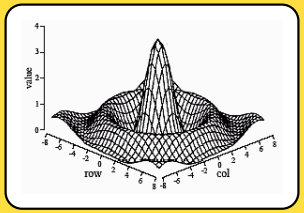

Spectral

Box-filtered DNS

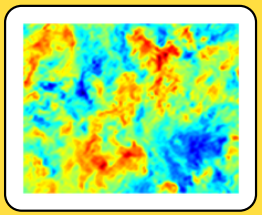

unfiltered

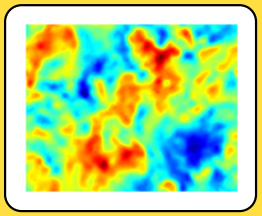

filtered (narrow)

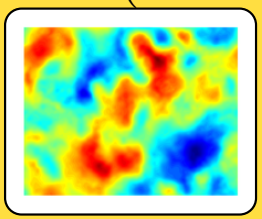

filtered (wide)

Gaussian-blurred image

Explicit Filter Operators For High-Order FR Schemes

1D High-Order Element, $\xi = [-1 : 1]$

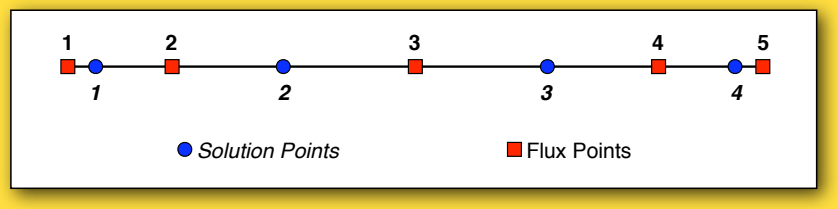

Explicit Filter Operators For High-Order FR Schemes

1D High-Order Element, $\xi = [-1 : 1]$

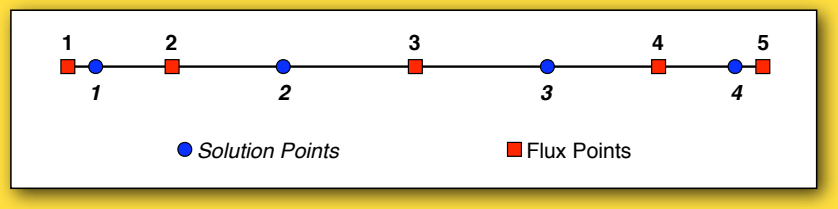

Specification

- Limit kernel to element interior for compactness/parallelisability
- Asymmetric filter kernel
- Well-defined physical/spectral cutoff
- Consistent behaviour for different N

Explicit Filter Operators For High-Order FR Schemes

1D High-Order Element, $\xi = [-1 : 1]$

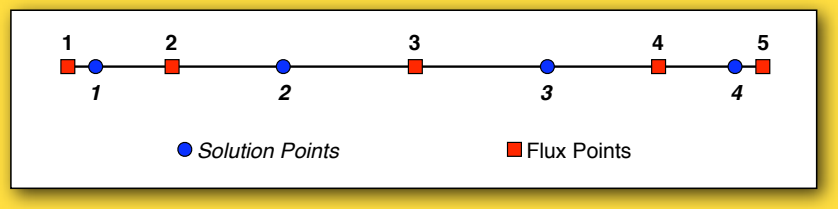

Specification

- Limit kernel to element interior for compactness/parallelisability
- Asymmetric filter kernel
- Well-defined physical/spectral cutoff
- Consistent behaviour for different N

Generic Discrete Nodal Filter

- Weighted sum over N nodes:

$$\overline{u}_i(\xi) = \int_{-\infty}^{\infty} F(\xi_i - \xi) u(\xi) d\xi$$

$$\approx \sum_{j=1}^{N} w_{ij} u_j, \quad (i = 1, \ldots, N)$$

- Filter kernel F has a characteristic filter width $\overline{\triangle}$
- Transfer function measures effect on spectrum

Constrained Discrete Filter 1 (CD1)

- Integrate Gaussian filter kernel over Gauss-Legendre quadrature points:

$$\overline{u}_i(x) \approx K \sum_{j=1}^{N} w_i^G u_j \exp\left[-6(\beta_{ij})^2\right], \quad \beta_{ij} = (\xi_i - \xi_j)/\overline{\triangle}, \quad \overline{\triangle}_i = \alpha_i \triangle$$

- w_i^G = Gauss quadrature weights, $\alpha_s = 1.5$ = filter width ratio, $\triangle = 2/N$

Lodato et al. (2012), Int. J. Num. Meth. Fl.

Constrained Discrete Filter 1 (CD1)

- Integrate Gaussian filter kernel over Gauss-Legendre quadrature points:

$$\overline{u}_i(x) \approx K \sum_{j=1}^{N} w_i^G u_j \exp\left[-6(\beta_{ij})^2\right], \quad \beta_{ij} = (\xi_i - \xi_j)/\overline{\triangle}, \quad \overline{\triangle}_i = \alpha_i \triangle$$

- w_i^G = Gauss quadrature weights, $\alpha_s = 1.5$ = filter width ratio, $\triangle = 2/N$

Transfer function of CD1 for $N = 3, 4, 5$

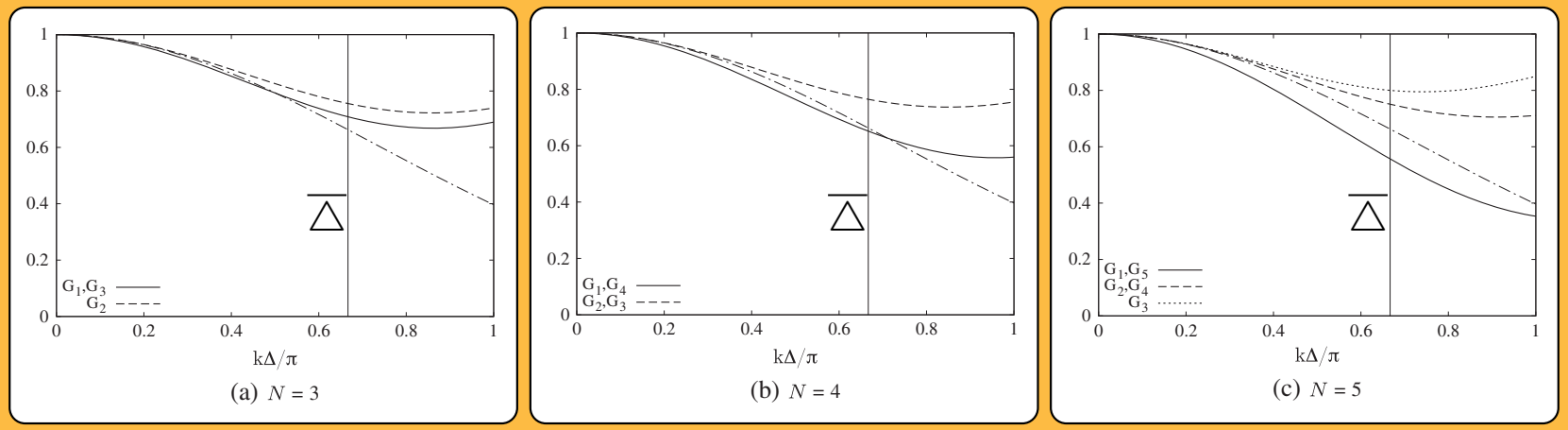

(a) $N = 3$ (b) $N = 4$ (c) $N = 5$

Lodato et al. (2012), Int. J. Num. Meth. Fl.

Constrained Discrete Filter 2 (CD2)

- Can be applied to arbitrarily spaced points
- Based on high-order-commuting filters of Vasilyev et al (1998)
- Determine N weights w_i^s for s^{th} node from N constraints:

  1. Weights sum to 1;
  2. Cutoff lengthscale $\overline{\triangle} = \alpha\triangle$;
  3, ..., N. Enforce $(N-1)^{\text{th}}$-order filtering error

Lodato et al. (2012), Int. J. Num. Meth. Fl.

Constrained Discrete Filter 2 (CD2)

- Can be applied to arbitrarily spaced points
- Based on high-order-commuting filters of Vasilyev et al (1998)
- Determine N weights w_i^s for s^{th} node from N constraints:

  1. Weights sum to 1;
  2. Cutoff lengthscale $\overline{\triangle} = \alpha\triangle$;
  3, ..., N. Enforce $(N-1)^{\text{th}}$-order filtering error

Transfer function of CD2 for $N = 3, 4, 5$

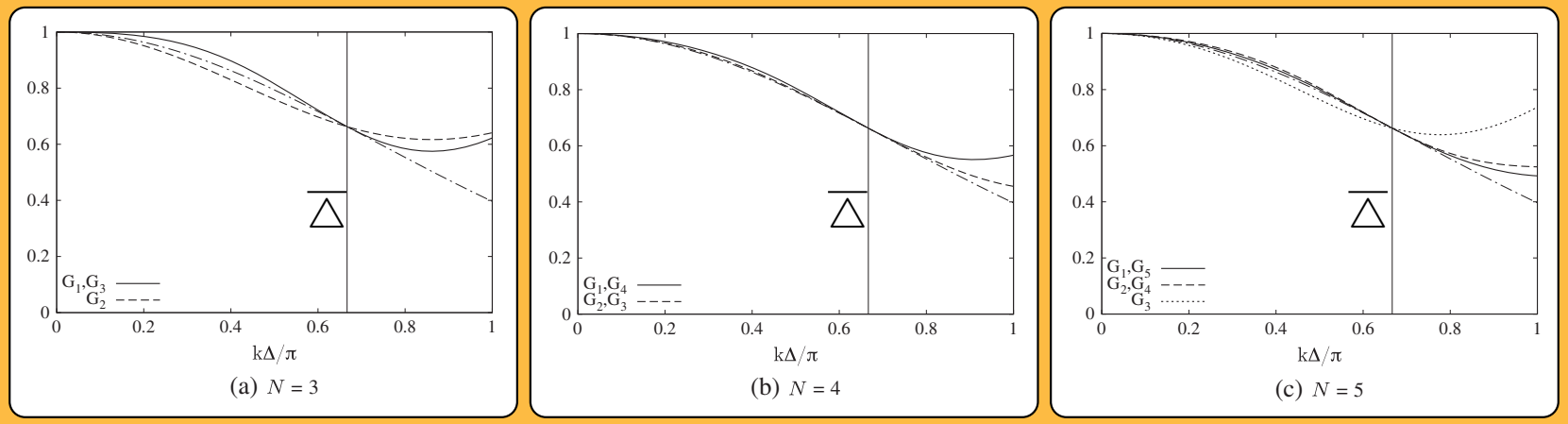

(a) $N = 3$ (b) $N = 4$ (c) $N = 5$

Lodato et al. (2012), Int. J. Num. Meth. Fl.

Pseudo-Spectral Methods and Modal Filtering

- VCJH schemes use Legendre polynomials $\phi(\xi)$ to represent a pseudo-spectrum
- Define modal solution as:

$$u_j(\xi) = \sum_{k=1}^{N} \hat{u}_{j,k}\phi_k(\xi)$$

- $\hat{u}_{j,k}$ = modal solution coefficients
- Can use a modal filter to damp high-order modes (short wavelengths)[1]

Legendre polynomials

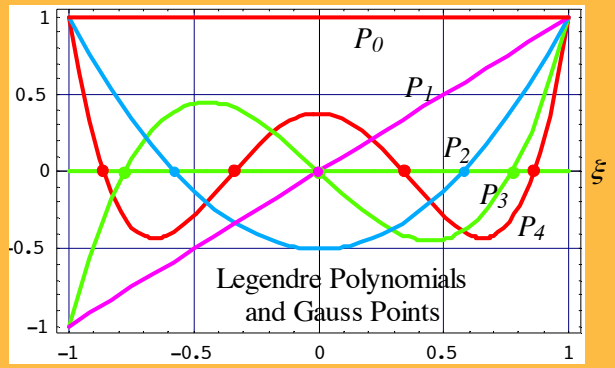

[1] Metais & Lesieur (1992), J. Fl Mech. 239. [2] Blackburn & Schmidt (2003), J. Comp. Phys. 186. [3] Lodato et al. (2012), Int. J. Num. Meth. Fl. [4] Presamuthan et al. (2009), AIAA P.

Pseudo-Spectral Methods and Modal Filtering

- VCJH schemes use Legendre polynomials $\phi(\xi)$ to represent a pseudo-spectrum
- Define modal solution as:

$$u_j(\xi) = \sum_{k=1}^{N} \hat{u}_{j,k}\phi_k(\xi)$$

- $\hat{u}_{j,k}$ = modal solution coefficients
- Can use a modal filter to damp high-order modes (short wavelengths)[1]

Legendre polynomials

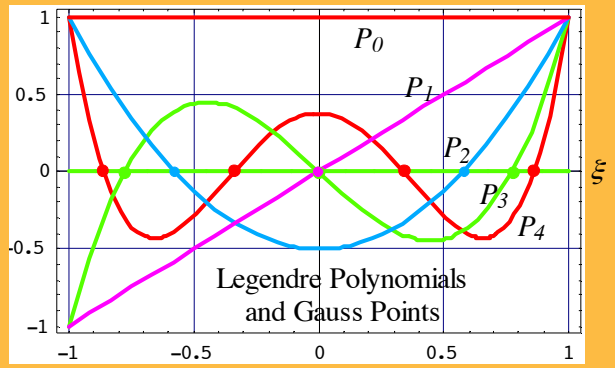

Restriction-Prolongation (RP) or sharp modal cutoff filter[2,3,4]

(1). 'Restrict' (aggregate) solution to lower-order basis

(2). 'Prolongate' (interpolate) solution back to original basis.

[1] Metais & Lesieur (1992), J. Fl Mech. 239. [2] Blackburn & Schmidt (2003), J. Comp. Phys. 186. [3] Lodato et al. (2012), Int. J. Num. Meth. Fl. [4] Presamuthan et al. (2009), AIAA P.

RP Filter Behaviour

- Gaussian curves in black for comparison
- Varying $\overline{\triangle}$ across element
- Transfer function > 1: amplification at points near element interfaces

Lodato et al. (2012), Int. J. Num. Meth. Fl.

Transfer function of RP filter for $N = 3, 4, 5, 6$

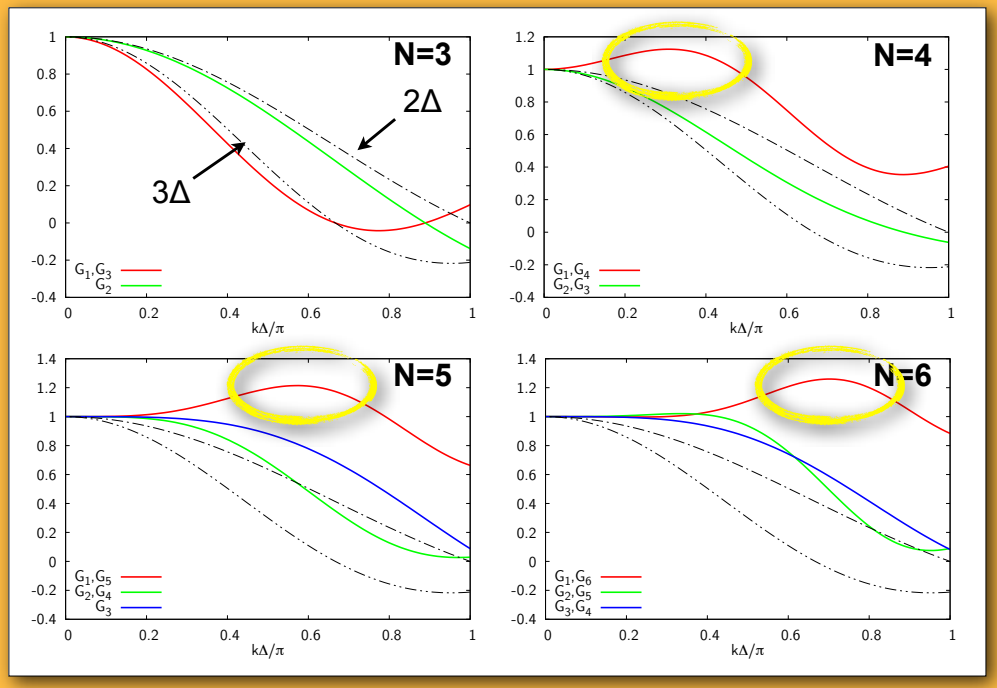

Comparison of Filters in LES of Turbulent Channel Flow

- Filtering extended to 2D and 3D (quadrilateral/hexahedral elements) by tensor products

Lodato et al. (2012), Int. J. Num. Meth. Fl.; Lodato, Castonguay, Jameson (2011), CTR Annual Research Briefs; Moser, et al. (1999), Phys. Fluids, 11(4)

Comparison of Filters in LES of Turbulent Channel Flow

- Filtering extended to 2D and 3D (quadrilateral/hexahedral elements) by tensor products

- Turbulent channel flow, $Re_\tau = 395$
- Compared to DNS of Moser et al.
- 4th-order-accurate SD scheme (N=4)
- WSM with (○) CD1, (×) CD2, (•) RP filters
- Element interfaces shown by vertical dotted lines

Lodato et al. (2012), Int. J. Num. Meth. Fl.; Lodato, Castonguay, Jameson (2011), CTR Annual Research Briefs; Moser, et al. (1999), Phys. Fluids, 11(4)

Comparison of Filters in LES of Turbulent Channel Flow

- Filtering extended to 2D and 3D (quadrilateral/hexahedral elements) by tensor products

- Turbulent channel flow, $Re_\tau = 395$
- Compared to DNS of Moser et al.
- 4th-order-accurate SD scheme (N=4)
- WSM with (○) CD1, (×) CD2, (•) RP filters
- Element interfaces shown by vertical dotted lines

Lodato et al. (2012), Int. J. Num. Meth. Fl.; Lodato, Castonguay, Jameson (2011), CTR Annual Research Briefs; Moser, et al. (1999), Phys. Fluids, 11(4)

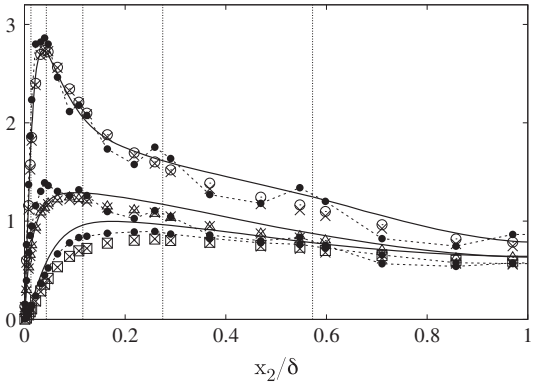

(c) $u^*_{1\mathrm{rms}}$ (○), $u^*_{2\mathrm{rms}}$ (□), $u^*_{3\mathrm{rms}}$ (△)

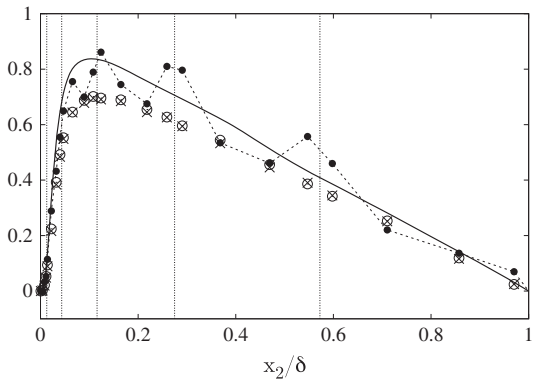

(d) $-\langle u^*_1 u^*_2 \rangle$

LES of Flow Past a Square Cylinder at Re = 21400

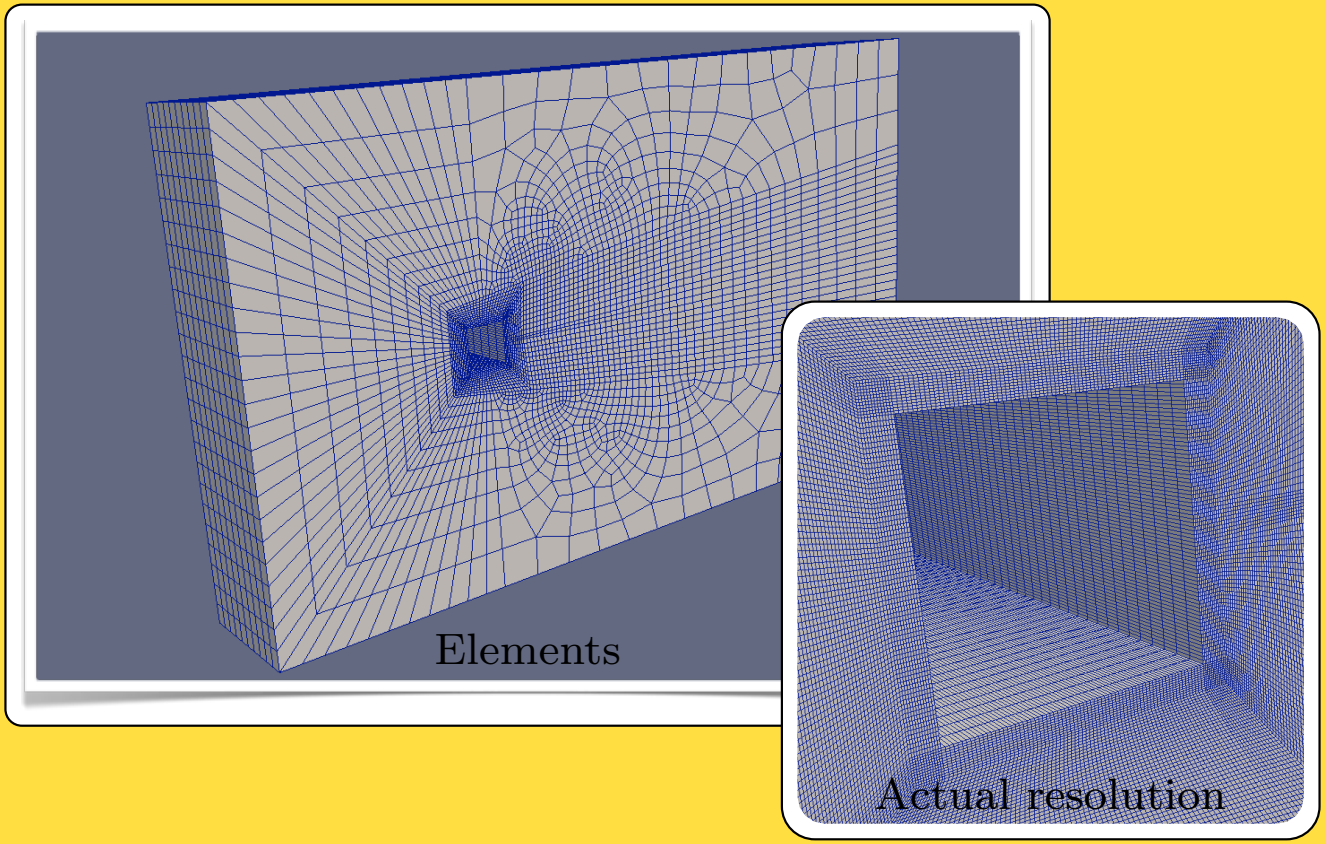

- SGS model: WSM model, CD2 filter
- Numerical scheme: Spectral Difference, 4rd order accurate
- Time integration: 3rd order Runge Kutta
- No. of elements: 35760 (2.3×10^6 DoF)
- Grid dimensions: $21D \times 12D \times 3.2D$
- Mach: 0.3

Lodato and Jameson (2012), 7th Int. Conf. CFD, Hawaii

LES of Flow Past a Square Cylinder at Re = 21400

Isosurfaces of Q criterion

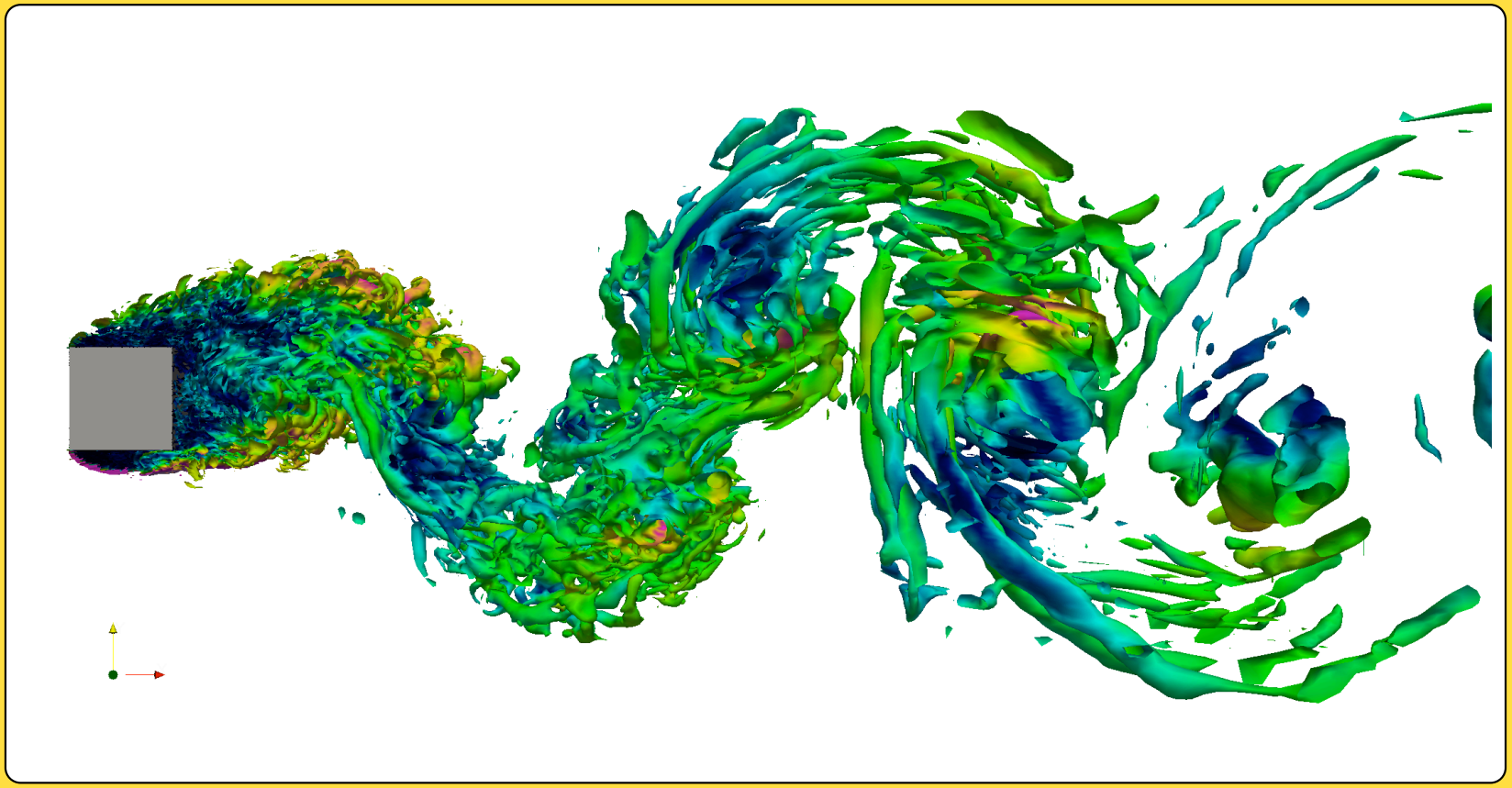

Lodato and Jameson (2012), 7th Int. Conf. CFD, Hawaii

LES of Flow Past a Square Cylinder at Re = 21400

Mean velocity and second moments in cylinder wake

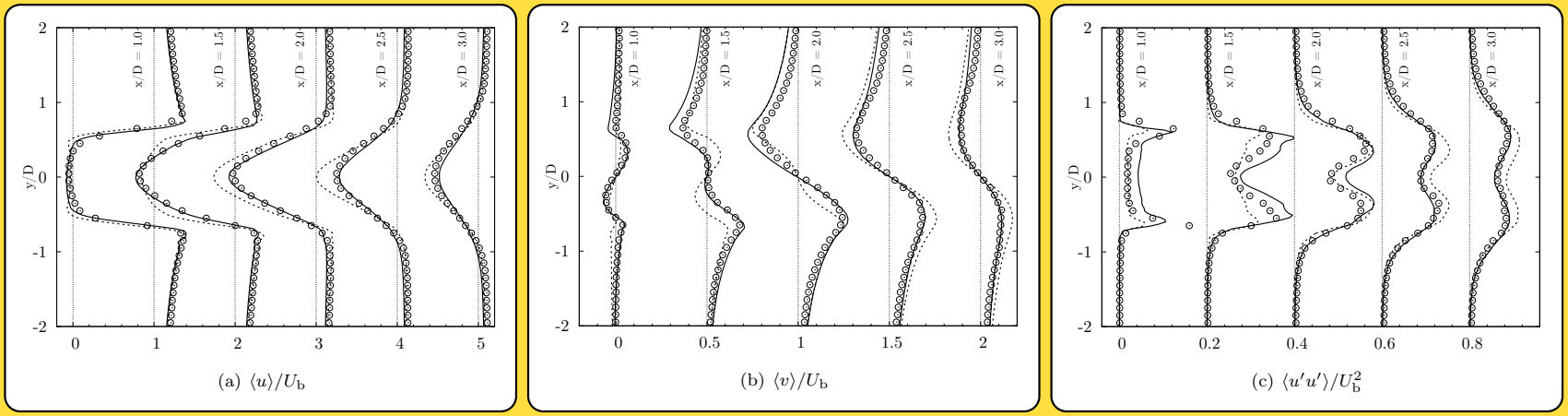

- ○ experimental data, — SD with WSM model, . . . SD without WSM model

Effect of using LES Model

- SD alone was unsatisfactory in these under-resolved computations
- SD + SGS significantly improved accuracy of mean velocity
- Less improvement in accuracy of second moments
- SD + SGS on finer mesh (not shown) – much better second moment accuracy
- At higher *Re*, hard to avoid under-resolution – SGS model is essential

Lodato and Jameson (2012), 7th Int. Conf. CFD, Hawaii

Nodal Filters on Triangles

Generic triangular kernel

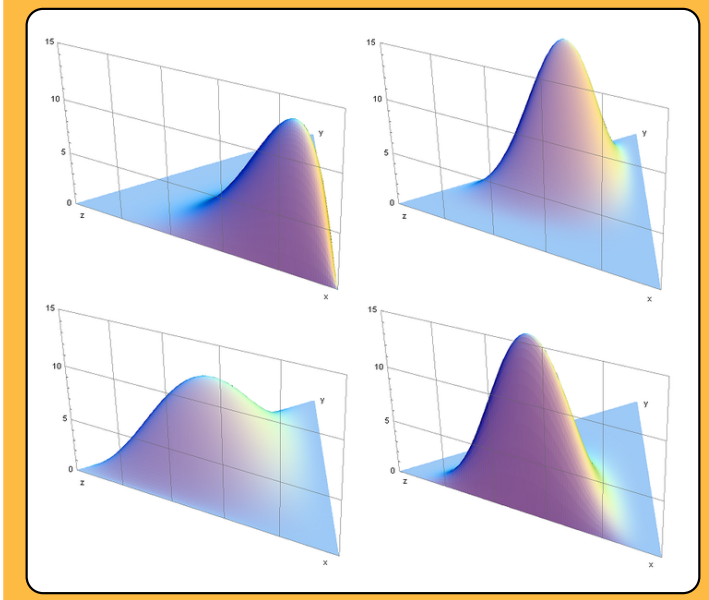

- At each solution point, filter is a weighted sum over all points

Nodal Filters on Triangles

Generic triangular kernel

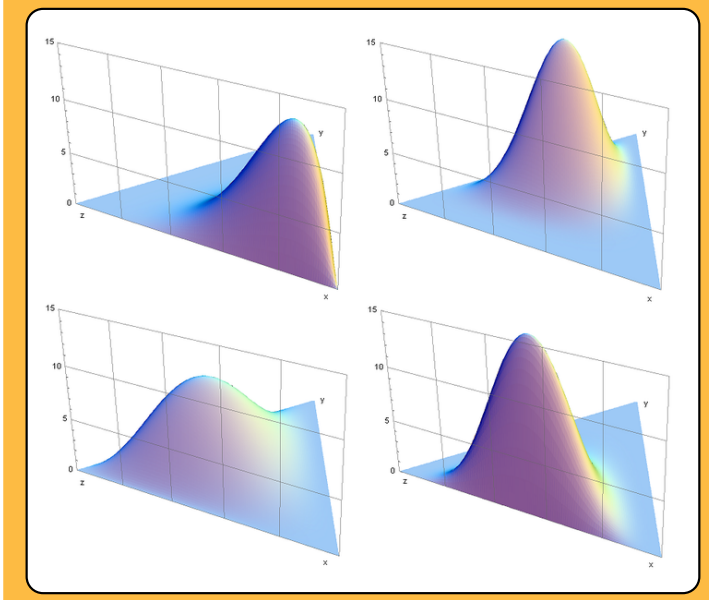

- At each solution point, filter is a weighted sum over all points

- Apply CD1/CD2 nodal filters to N triangle quadrature points
- Define filter kernel in radial coordinates:

$$r_j^s = (1/\overline{\triangle})\sqrt{(\xi_j - \xi_s)^2 + (\eta_j - \eta_s)^2)}$$

- What is the appropriate definition of $\overline{\triangle}$?
- How will their transfer functions behave?
- Currently investigating properties

Extension of 1D Modal Filters to Triangles

- Tensor product not applicable to simplices (triangles, tetrahedra)
- Dubiner basis: warped product of Jacobi polynomials
- Apply modal filter to Dubiner modes

Extension of 1D Modal Filters to Triangles

- Tensor product not applicable to simplices (triangles, tetrahedra)
- Dubiner basis: warped product of Jacobi polynomials
- Apply modal filter to Dubiner modes

Dubiner transformation $[-1,1]^2 \rightarrow \mathbf{T}^2$

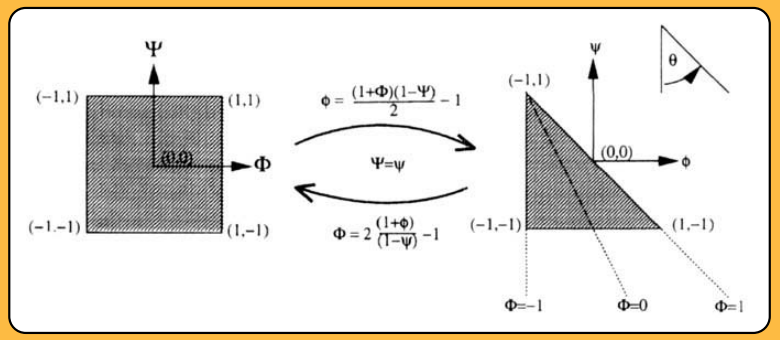

Sherwin and Karniadakis (1995)

Extension of 1D Modal Filters to Triangles

- Tensor product not applicable to simplices (triangles, tetrahedra)
- Dubiner basis: warped product of Jacobi polynomials
- Apply modal filter to Dubiner modes

Dubiner transformation $[-1,1]^2 \rightarrow \mathbf{T}^2$

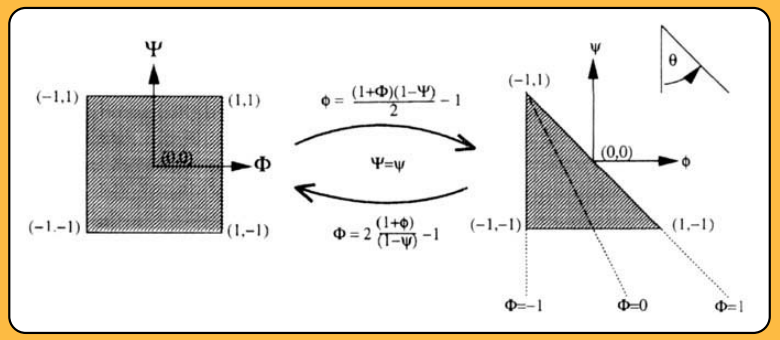

Sherwin and Karniadakis (1995)

Dubiner transformation $[-1,1]^3 \rightarrow \mathbf{T}^3$

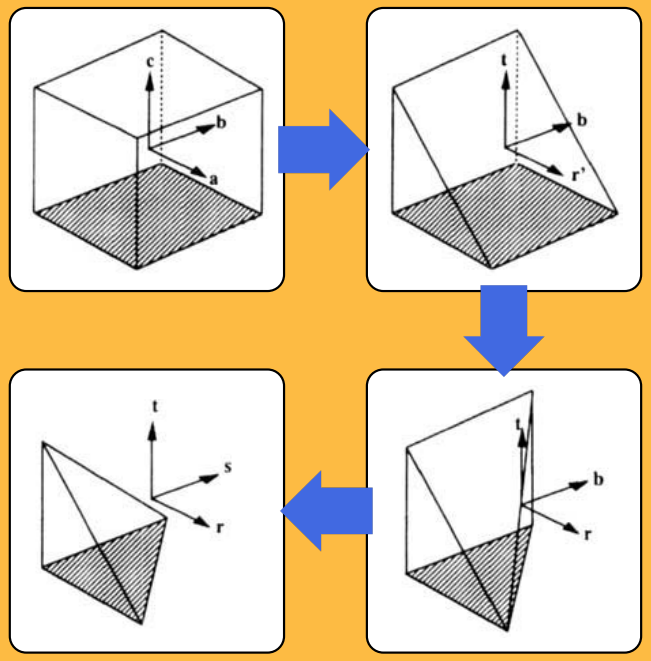

Li and Wang (2010)

Other Modal Filters

Illustration of generic modal filter[1]

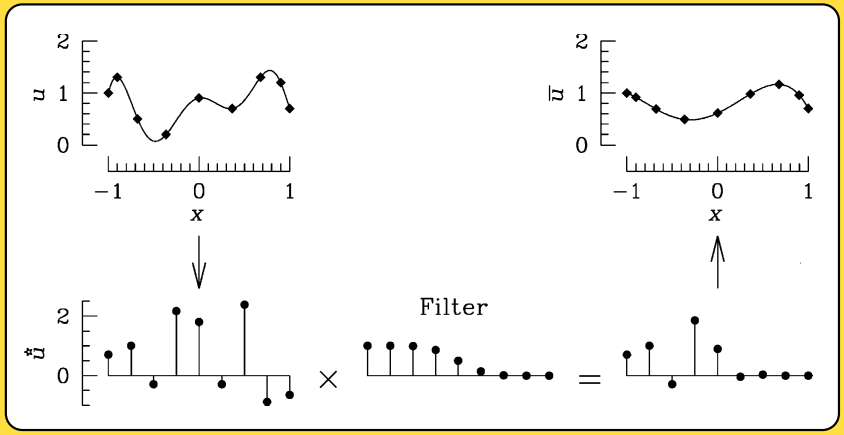

[1] Blackburn & Schmidt (2003), J. Comp. Phys. 186. [2] Bouffanais et al. (2006), J. Sci. Comp. 27(1-3). [3] Boyd (1996).

Other Modal Filters

Illustration of generic modal filter[1]

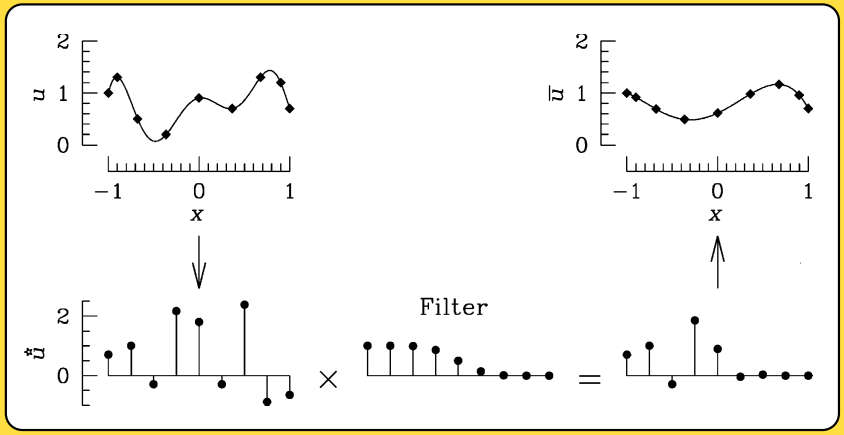

[1] Blackburn & Schmidt (2003), J. Comp. Phys. 186. [2] Bouffanais et al. (2006), J. Sci. Comp. 27(1-3). [3] Boyd (1996).

Examples

Name	Filter $\hat{F}$
Box	$\frac{\sin(0.5\pi k/k_c)}{0.5\pi k/k_c}$
Gaussian	$\exp\left(\frac{-(\pi k/k_c)^2}{24}\right)$
Bouffanais[2]	$\frac{1}{1+(k/k_c)^2}$
Boyd-Vandeven[3]	...

Modal Filter Behaviours

Transfer function of Gaussian, Box and Boyd-Vandeven Modal Filters for $N = 3$

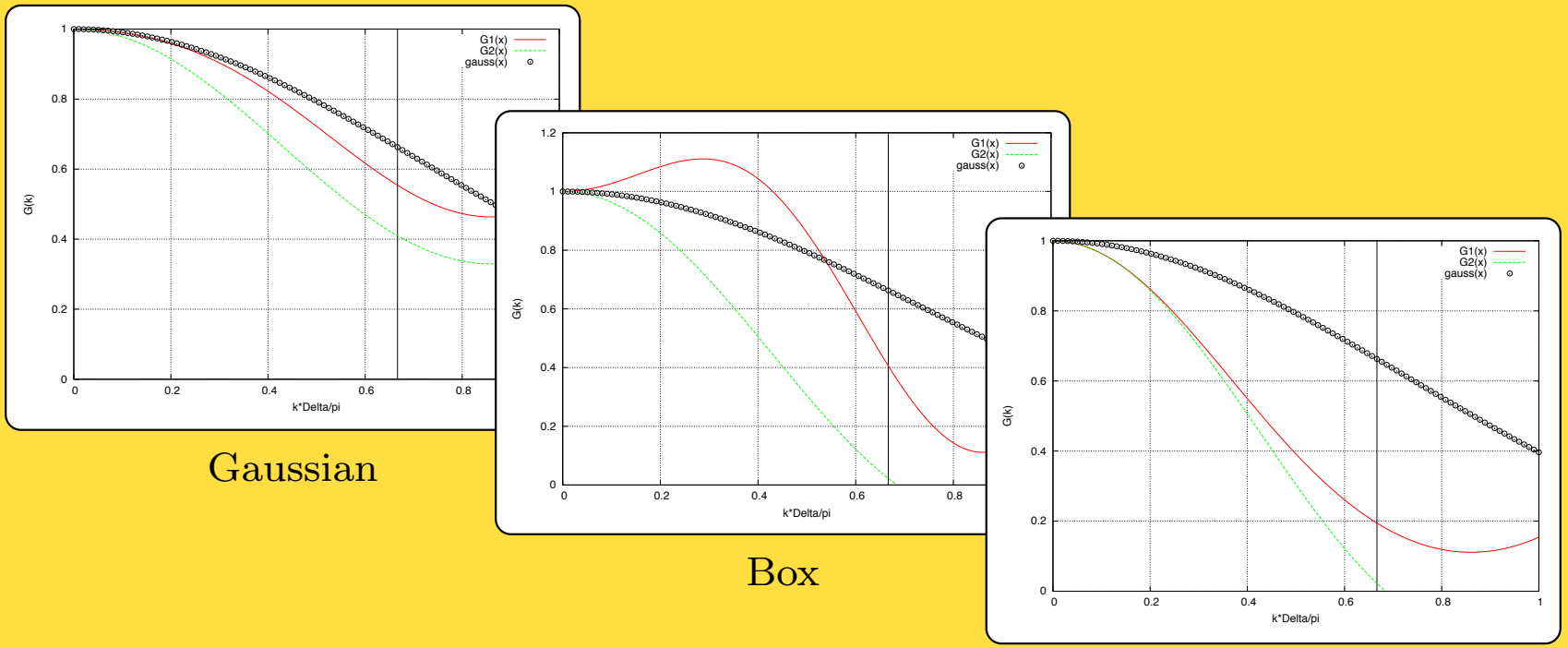

Gaussian

Box

Boyd-Vandeven

- Gaussian and Boyd-Vandeven filters show well-behaved transfer functions

Hyperviscosity and Modal Filtering

Spectral Vanishing Viscosity (SVV)[1]

- In 1D, add 'hyperviscosity' with strength ϵ_N to damp aliasing instability:

$$\frac{\partial u_h}{\partial t} + \frac{\partial}{\partial x}(f(u_h)) = \epsilon_N (-1)^{p+1} \frac{\partial^{2p}}{\partial x^{2p}} u_h, \quad \epsilon_N = C_p / N^{2p-1}, \tag{2}$$

[1] Tadmor (1989), SIAM J. Numer. Anal. 26(1).
[2] Gottlieb & Hesthaven (2001), J. Comp. Appl. Math. 128
[3] Meister et al. (2009), Math. Schriften Kassel.

Hyperviscosity and Modal Filtering

Spectral Vanishing Viscosity (SVV)[1]

- In 1D, add 'hyperviscosity' with strength ϵ_N to damp aliasing instability:

$$\frac{\partial u_h}{\partial t} + \frac{\partial}{\partial x}(f(u_h)) = \epsilon_N (-1)^{p+1} \frac{\partial^{2p}}{\partial x^{2p}} u_h, \quad \epsilon_N = C_p / N^{2p-1}, \tag{2}$$

SVV as a Modal Filter[2]

- (2) is equivalent to applying an exponential modal filter to solution:

$$\overline{u} \quad = \sum_{|k|<N} \sigma(k/N) \hat{u}_k e^{ikx}, \quad \sigma(\eta) = \exp(-C_p N \Delta t \eta^{2p}) \tag{3}$$

- σ is exponential filter of order $2p$ and strength $\alpha = C_p N \Delta t$
- Choose C_p so that α is constant for different N (Δt depends on N)
- Similar expression can be derived for Dubiner basis[3]

[1] Tadmor (1989), SIAM J. Numer. Anal. 26(1).
[2] Gottlieb & Hesthaven (2001), J. Comp. Appl. Math. 128
[3] Meister et al. (2009), Math. Schriften Kassel.

Connections Between Filtering, SGS Modeling and Stabilisation

- Stability of VCJH schemes due to implicitly containing an SVV-type term
- SVV term is purely dissipative - cannot model complex SGS physics
- Still need an SGS model e.g. WSM
- Investigating use of SVV-type modal filter as explicit filter in SGS model

Stabilisation

High-order Filter ⟷ SGS model

Connections Between Filtering, SGS Modeling and Stabilisation

- Stability of VCJH schemes due to implicitly containing an SVV-type term
- SVV term is purely dissipative - cannot model complex SGS physics
- Still need an SGS model e.g. WSM
- Investigating use of SVV-type modal filter as explicit filter in SGS model

Stabilisation

High-order Filter ⟷ SGS model

- Some combination of filtering, stabilisation and SGS modeling techniques will result in a stable and accurate method for real-world high-Re turbulent flows!

Summary and Future Directions

Summary

- Need unstructured meshes, high-order numerics and LES modeling to simulate complex problems at realistic Reynolds numbers
- Developing explicit modal and nodal filters on triangles and tetrahedra
- Investigating SGS models appropriate for high-order schemes

Summary and Future Directions

Summary

- Need unstructured meshes, high-order numerics and LES modeling to simulate complex problems at realistic Reynolds numbers
- Developing explicit modal and nodal filters on triangles and tetrahedra
- Investigating SGS models appropriate for high-order schemes

ACL Activities

- Developing an open-source high-order LES code
- Extending family of energy-stable Flux Reconstruction (VCJH) schemes
- Hybrid RANS/LES modeling
- Implicit timestepping
- Polynomial adaptivity (increase/decrease polynomial order)
- Polynomial multigrid convergence acceleration
- Moving meshes

Acknowledgements

The presented research is a combined effort by...

- Principal Investigator: Professor Antony Jameson
- Postdocs: Jonathan Bull, Guido Lodato, Peter Vincent
- PhD students: David Williams, Manuel R. Lopez Morales, Andy Chan, Patrice Castonguay, Yves Alleneau, Kui Ou, Sachin Presamuthan

It was made possible by the generous support of...

- The Airforce Office of Scientific Research under grant FA9550-10-1-0418 by Dr. Fariba Fahroo
- The National Science Foundation under grants 0708071 and 0915006 monitored by Dr. Leland Jameson

Thank you for listening